Clouds and Shortwave Fluxes at Nauru. Part I: Retrieved Cloud Properties

SALLY A. MCFARLANE AND K. FRANKLIN EVANS

Program in Atmospheric and Oceanic Sciences, University of Colorado, Boulder, Colorado

(Manuscript received 9 January 2003, in final form 1 July 2003)

ABSTRACT

The datasets currently being collected at the Atmospheric Radiation Measurement (ARM) program's sites on the islands of Nauru and Manus represent the longest time series of ground-based cloud measurements available in the tropical western Pacific region. In this and a companion paper, a shortwave flux closure study is presented using observations collected at the Nauru site between June 1999 and May 2000. This paper presents frequency of occurrence of nonprecipitating liquid and ice clouds detected by the millimeter wavelength cloud radar (MMCR) and statistics of retrieved microphysical properties. The companion paper presents results from a closure study in which the retrieved cloud properties are input to a radiative transfer model, and the modeled surface fluxes are compared to observations. The liquid cloud properties are retrieved from MMCR and microwave radiometer (MWR) measurements using a Bayesian retrieval technique. Properties of ice phase clouds are retrieved from MMCR measurements using regression equations based on in situ observations taken during the Central Equatorial Pacific Experiment (CEPEX). Nonprecipitating liquid clouds were observed at Nauru in 35% of the radar observations. These clouds were primarily shallow cumulus with bases less than 1 km. Of the retrieved liquid clouds, 90% had liquid water path less than 100 g m^{-2}. The average retrieved effective radius was 7.5 μm. The frequency of liquid cloud detection and height of the liquid cloud base showed a clear diurnal cycle, which is most likely related to the island effect and the existence of the Nauru cloud plume. Ice clouds with no underlying liquid clouds were detected in 16.5% of the radar observations and ice clouds above liquid clouds in 7.7% of the observations. The mean retrieved IWP of the radar-detected ice clouds was 22.1 g m^{-2}, and the mean effective diameter retrieved was 72 μm. Large monthly variability was seen in both the amount of cirrus detected and the retrieved ice water path. Ice clouds were observed by the radar more frequently at night than during the day at Nauru, but there was no clear diurnal trend in the retrieved microphysical properties.

1. Introduction

The tropical western Pacific (TWP) region has long been known to be important to global climate (Webster and Lukas 1992). The warm pool region has the highest average sea surface temperatures and most intense convection in any oceanic region, as well as strong atmospheric–ocean coupling due to the net fresh water flux into the ocean from precipitation and the strong solar radiative heating. The variability of cloudiness over the warm pool region has a large impact on atmospheric heating rates and solar radiative flux at the ocean surface, which influence atmospheric circulations.

Due to the remote location and difficulty in establishing observational platforms, there are few ground-based observations of surface radiation and cloud properties in the TWP region. The Tropical Ocean Global Atmosphere Coupled Ocean–Atmosphere Response Experiment (TOGA COARE) was conducted from November 1992 through February 1993 in the western Pacific region bordered by 10°N–10°S, 140°E–180°, with an intensive observational region centered at 2°S, 156°E (Webster and Lukas 1992; Webster et al. 1996). Surface downwelling shortwave and infrared irradiance were measured from ground sites, ocean buoys, and research ships.

The Pilot Radiation Observation Experiment (PROBE) was conducted in Kavieng, Papua New Guinea, from 6 January–28 February 1993 as part of the TOGA COARE field project. In addition to radiometric instruments, the instrumentation at the Kavieng site included a sun photometer, micropulse lidar, and a dual channel microwave radiometer (Westwater et al. 1999). The Central Equatorial Pacific Experiment (CEPEX) was conducted during March and April 1993 in the central and eastern equatorial Pacific. Measurements of irradiance at the tropopause were taken by the National Aeronautics and Space Administration (NASA) ER-2 aircraft, surface fluxes were measured by the National Oceanic and Atmospheric Administration (NOAA) Lockheed P-3 aircraft and the the ship R/V *John Vickers*, and in situ cloud measurements were taken by the Aeromet Learjet (McFarquhar and Heymsfield 1996).

In recent years, the Department of Energy's Atmo-

Corresponding author address: Dr. Sally A. McFarlane, Pacific Northwest National Laboratory, P.O. Box 999/MS K9-24, Richland, WA 99352.
E-mail: Sally.McFarlane@pnl.gov

spheric Radiation Measurement (ARM) program has developed two measurement sites on the islands of Nauru and Manus in the tropical warm pool region. The development of these sites offers the first opportunity in the tropical western Pacific for long-term datasets from which cloud microphysical properties and the parameters of the surface radiation budget can be retrieved. The island republic of Nauru, is located at 0.5°S, 166.9°E, on the eastern edge of the warm pool and in the marine trade cumulus region. The trade cumulus region is important to climate both dynamically and radiatively. These shallow cumulus clouds act to transport heat, momentum, moisture, and pollutants from the boundary layer to the troposphere, and help maintain the trade inversion (Duynkerke 1998; Albrecht 1981). Radiatively, they are important because the amount of net solar radiation reaching the surface in the trade cumulus region (which is controlled by the cloud amount and microphysical properties of the trade cumulus) may affect sea surface temperatures (Albrecht 1981). Randall et al. (1998) states that ''Because the tradewind regime is so wide-spread, its accurate simulation is very important for coupled ocean–atmosphere modeling. Unfortunately, physically based parameterizations of tradewind cumulus clouds, designed for use in AGCMs, [Atmospheric General Circulation Models] are currently at a very primitive stage.''

In order to improve model parameterizations in this region, statistics of cloud macrophysical and microphysical properties are needed. However, the idea that a time series of vertical observations at a single point is representative of the average cloud properties in a GCM grid box needs further examination. Cloud properties retrieved from remote sensing instrumentation are usually validated by comparing against in situ aircraft measurements. However, issues exist with these comparisons including large volume sampling discrepancies, uncertainties of in situ cloud probes, and few data points for comparisons (Sassen et al. 1999). Since a primary quantity of interest to climate modelers is the radiative budget, an important question to consider is whether the cloud properties retrieved from remote sensing measurements are consistent with the radiative budget. Can the retrieved optical properties of the clouds be used to accurately predict the effect of clouds on the radiation field?

In this set of papers, we present a broadband shortwave flux closure experiment at the ARM site on Nauru. The motivation for the study is to explore whether time series of cloud properties retrieved from a vertically pointing radar and microwave radiometer at a fixed location are statistically consistent with the observed surface radiation. In this paper (hereafter Part I), we present the statistics of cloud occurrence and retrieved properties of nonprecipitating clouds at Nauru. In the comparison paper (McFarlane and Evans 2004, submitted to *J. Atmos. Sci.*; hereafter Part II), we input the retrieved cloud properties into a radiative transfer model, calculate the downwelling shortwave flux at the surface, and compare the modeled and observed flux. If consistency is found between the modeled and observed fluxes, then the time series of retrieved properties can be considered to represent the real cloud properties in a radiatively consistent manner.

In section 2 of this paper, we describe the measurements taken at Nauru and give a brief description of the cloud property retrieval methods. In section 3 we present the cloud property statistics and in section 4, we discuss diurnal variability in the retrieved properties.

2. Observations and retrieval techniques

The Atmospheric Radiation and Cloud Station (ARCS; Mather et al. 1998) at Nauru became fully operational in December 1998. Details of the instruments and measurements from the ARCS used in this study are discussed below. Data from the instruments at the Nauru ARCS site are freely available to the scientific community from the ARM archive (available online at http://www.archive.arm.gov). We use a dataset consisting of observations taken between 1 June 1999 and 31 May 2000.

We derive statistics on cloud frequency of occurrence and cloud-base and cloud-top heights from the millimeter wave cloud radar (MMCR), which is a vertically pointing Doppler radar that operates at 34.86 GHz (8.6 mm; Moran et al. 1997). Details of the operational parameters of the MMCR at each ARM site are given in Clothiaux et al. (1999). We use radar reflectivity values from the Active Remote Sensing of Cloud Layers (ARSCL) product described in Clothiaux et al. (2000), which combines information from all modes of the MMCR to produce a best estimate of hydrometeor reflectivities at 10-s temporal and 45-m vertical resolution. Although use of the micropulse lidar (MPL) would improve the accuracy of the cloud-base and cloud-top height retrievals, the MPL laser substantially lost power in November 1999 and failed completely on 16 January 2000. It was not returned to service until 17 October 2000. For consistency within the dataset, we opted not to use any MPL data. In section 2b, we present further discussion of the effect on the retrieved statistics of using only the radar to determine cloud existence and boundaries.

Accurate determination of cloud phase is difficult without a polarization lidar. Therefore, we classify cloud phase based on a simple temperature threshold. Clouds with top temperatures greater than or equal to −10°C are assumed to be liquid clouds, while all other clouds are assumed to be ice clouds. Temperature is determined from the nearest radiosonde launch. Properties of ice clouds are retrieved from the radar reflectivity, while properties of liquid clouds are retrieved from combining the radar reflectivity measurements with measurements from a microwave radiometer (MWR). The MWR is a dual-channel radiometer that measures atmospheric brightness temperatures at the wavelengths of 23.8 and

31.4 GHz. The MWR is calibrated by an automated tipping curve calibration, which can provide absolute accuracy of about 0.5 K if performed correctly (Han and Westwater 2000). Westwater et al. (2003) showed that the MWR was well calibrated during the Nauru99 field experiment (15 June–15 July 1999) with the accuracy of the brightness temperatures within ± 1 K. An uncertainty of 1 K corresponds to roughly 30 g m^{-2} in liquid water path.

a. Liquid cloud retrievals

In recent years, due primarily to the development of highly sensitive cloud radars, many algorithms for retrieving cloud optical properties from ground-based remote sensing observations have been developed for liquid clouds (Frisch et al. 1995, 1998; Dong et al. 1997; Mace and Sassen 2000). However, few of these liquid cloud retrievals are appropriate for the trade cumulus regime prevalent at Nauru as these algorithms were developed specifically for stratus and stratocumulus clouds. Additionally, these methods do not account for uncertainty in the inputs to the algorithm, which is especially important for shallow clouds, where the MWR is at the limit of its sensitivity. The algorithms developed by Dong et al. (1997) and Mace and Sassen (2000) are constrained by the observed shortwave radiation at the surface. While guaranteeing that the retrieved properties will be consistent with the surface radiation, such constraints assume completely overcast conditions, which are rarely seen at Nauru.

A Bayesian retrieval algorithm developed by McFarlane et al. (2002) was designed to alleviate some of the above issues. In this method, Bayes' theorem of conditional probability is used to relate the inverse problem to the forward problem through the set of remote sensing observations and prior knowledge of cloud microphysics. Bayes' theorem of conditional probability is given by

$$p_{\text{post}}(\mathbf{x}\,|\,\mathbf{y}) = \frac{p_f(\mathbf{y}\,|\,\mathbf{x})p_{\text{pr}}(\mathbf{x})}{\int p_f(\mathbf{y}\,|\,\mathbf{x})p_{\text{pr}}(\mathbf{x})\,d\mathbf{x}}, \tag{1}$$

where $\mathbf{y}$ is the measurement vector, or set of remote sensing observations (microwave brightness temperatures and vertical profiles of radar reflectivity), each with an associated measurement error, and $\mathbf{x}$ is the state vector, or set of all cloud and atmospheric parameters that affect the measurement vector.

In this equation, the quantity $p_{\text{pr}}(\mathbf{x})$, is known as the prior probability density function (pdf) of the state $\mathbf{x}$. It represents our knowledge about the possible values of $\mathbf{x}$ before the measurement is made. A prior pdf of the second, third, and sixth moments of the cloud droplet size distribution is developed from in situ aircraft measurements. These moments are chosen since radar reflectivity is related to the sixth moment of the size distribution, microwave brightness temperature is related to the vertical integral of the third moment, and visible extinction is related to the second moment.

The term, $p_f(\mathbf{y}\,|\,\mathbf{x})$, is the conditional, or forward, probability of the remote sensing observations $\mathbf{y}$, given the state vector. It is represented by a forward model that physically relates simulated values of the remote sensing observations (radar reflectivity, microwave brightness temperatures) to the moments of the droplet size distribution. The forward model includes information about vertical correlation of the radar reflectivities, uncertainties in the radar reflectivity and brightness temperature measurements, and a radiative transfer model to calculate the microwave absorption coefficients.

The denominator simply normalizes the integral. Finally, the term $p_{\text{post}}(\mathbf{x}\,|\,\mathbf{y})$ is known as the posterior pdf and is the probability distribution of the state vector given the measurement vector. The posterior pdf is the result of applying Bayes' theorem to a set of measurements and prior information. It represents our knowledge of the cloud properties after the measurements are taken, and includes information from the measurements and the prior pdf. The posterior pdf is obtained by combining the prior pdf and the forward model mathematically through Bayes' theorem. The retrieved cloud properties, including effective radius (r_e), liquid water content (LWC), and optical depth (τ), are the mean of the posterior pdf,

$$\langle \mathbf{x} \rangle = \frac{\int \mathbf{x} p_f(\mathbf{y}\,|\,\mathbf{x})p_{\text{pr}}(\mathbf{x})\,d\mathbf{x}}{\int p_f(\mathbf{y}\,|\,\mathbf{x})p_{\text{pr}}(\mathbf{x})\,d\mathbf{x}}, \tag{2}$$

and are calculated via a Monte Carlo integration. The standard deviation around the mean vector, $\sigma_{\mathbf{x}}$, which is an estimate of the uncertainty in the retrieved properties can also be calculated from

$$\sigma_{\mathbf{x}}^2 = \frac{\int (\mathbf{x} - \langle \mathbf{x} \rangle)^2 p_f(\mathbf{y}\,|\,\mathbf{x})p_{\text{pr}}(\mathbf{x})\,d\mathbf{x}}{\int p_f(\mathbf{y}\,|\,\mathbf{x})p_{\text{pr}}(\mathbf{x})\,d\mathbf{x}}. \tag{3}$$

The development of the prior and forward pdfs and the computation of the integrals are discussed in detail in McFarlane et al. (2002).

By using a pdf to describe the relation between the moments instead of constraining it to a fixed form, the algorithm is able to reproduce much of the variability in the relationship between the moments instead of only the average relationship. The Bayesian algorithm is flexible in that any type of liquid cloud regime could be used to create the prior pdf. In this case, we use size distributions from in situ measurements taken within shallow cumulus clouds during the Small Cumulus Mi-

crophysics Study (SCMS) and Joint Hawaiian Warm Rain Project (JHWRP) experiments (French et al. 2000; Raga et al. 1990). The Bayesian algorithm is applied only to nonprecipitating liquid clouds with reflectivities less than 0 dBZ (to avoid in-cloud drizzle contamination).

b. Ice cloud retrievals

Although combined radar and infrared radiometer methods (Matrosov et al. 1994; Mace et al. 1998) and lidar methods (Intrieri et al. 1993; Comstock and Sassen 2001; Wang and Sassen 2002) to retrieve cirrus microphysical properties are well established, they cannot be used if the cirrus is optically thick or lower clouds exist beneath the cirrus cloud. Recent algorithms that combine radar reflectivity and mean Doppler velocity (Matrosov et al. 2002; Mace et al. 2002) are promising for optically thick or multiple-layer clouds, but current results show a large percentage of cases where there is a weak relation between reflectivity and velocity, leading to poor performance of these algorithms.

Due to the difficulty in retrieving cloud properties robustly with more accurate, but more complicated, retrieval algorithms, we turn to a more basic retrieval method: regression equations as a function of radar reflectivity (Liao and Sassen 1994; Brown et al. 1995; Liu and Illingworth 2000). Although regression equations for ice water content (IWC) exist for tropical cirrus, no such equations were found in the literature for effective diameter in tropical cirrus. We developed regression equations for IWC and effective diameter D_e as a function of equivalent radar reflectivity (Z_e) and temperature using in situ data from the Aeromet Learjet during CEPEX (McFarquhar and Heymsfield 1996, 1997). The CEPEX experiment was designed in part to test the validity of the tropical thermostat mechanism proposed by Ramanathan and Collins (1991). The in situ observations primarily include measurements of outflow anvils in various stages of growth; the aircraft was only able to reach altitudes less than 14 km, so the tops of anvils and thin tropopause cirrus were not sampled (McFarquhar and Heymsfield 1996).

The dataset consists of almost 12 000 samples of processed 10-s-averaged two-dimensional cloud probe (2DC) data. The dataset contains particle concentration as a function of maximum diameter and area ratio. The data are binned into 28 bins in maximum diameter and 10 area ratio bins. Crystal habit, and therefore mass, are assigned to each bin based on the area ratio and maximum diameter (Heymsfield et al. 1990). For each bin, the diameter of a mass-equivalent sphere D_m is given by

$$D_{m,ij} = \left(\frac{6M_{ij}}{\pi\rho_{\text{ice}}}\right)^{1/3},$$

where i and j are the indices of the maximum diameter and area ratio bins, respectively, and ρ_{ice} is the density of solid ice.

The ice water content from particles with $D_m > 100$ is given by

$$\text{IWC}_{>100} = \sum_i \sum_j N(D_i, A_j)M_{ij},$$

where $N(D_i, A_j)$ is the number of particles per volume and M_{ij} the mass for size bin i and area ratio bin j. Heymsfield et al. (1990) estimate that this calculated IWC is accurate to within a factor of 2. The assignment of mass given the size and area ratio is based on midlatitude data, which may add additional uncertainty to the retrieval. However, McFarquhar and Heymsfield (1996) found agreement to within a factor of 2 between IWC calculated in this manner and IWC calculated with the method of Brown et al. (1995). For particles with diameters less than 100 μm, the 2DC measurements are not reliable, especially at the high airspeeds of the Learjet. McFarquhar and Heymsfield (1997) developed a parameterization for the IWC in ice crystals smaller than 100 μm from video ice particle sampler (VIPS) measurements. By iterating this equation in terms of the total IWC, the ice water content and number density of particles with $D_m < 100$ μm can be calculated.

The effective diameter is defined by Yang et al. (2000) as $D_e = (3/2)(V/A)$, where V is the volume and A the projected area. The volume and projected area are calculated for each bin of the 2DC data based on the assigned particle habit. The small crystals are assumed to be solid ice, so that volume is given by $V = (\pi/6)D_m^3$ and projected area by $A = (\pi/4)D_m^2$.

Based on calculations by Schneider and Stephens (1995), showing errors of less than 15% for particles with maximum dimensions up to 1400 μm at 8-mm wavelength, we assume that the Rayleigh approximation is valid and the equivalent radar reflectivity factor Z_e for each observation is given by

$$Z_e = \sum_i \sum_j \frac{|K_i|^2}{|K_w|^2} N_{>100}(D_i, A_j)D_m^6 + \sum_{D_m=0}^{100} \frac{|K_i|^2}{|K_w|^2} N_{<100}(D_m)D_m^6 \Delta D_m, \quad (4)$$

where ΔD_m is 5 μm. The coefficients K_i and K_w are functions of the refractive indices of ice and water, respectively. At 8.66 mm, $K_w^2 \approx 0.90$ and $K_i^2 \approx 0.18$ (Atlas et al. 1995). Matrosov et al. (1998) compared reflectivities measured by radar and calculated from measurements of droplet spectra during the First International Satellite Cloud Climatology Project (ISCCP) Regional Experiment II (FIRE-II) experiment and found general agreement with most differences <2 dB, which is near the level of the radar calibration. The calculated values of Z_e tended to be lower, possibly due to the undersampling of large particles by in situ probes and uncertainty in the particle mass derived from the in situ measurements.

Scatterplots of calculated IWC versus reflectivity and D_e versus reflectivity are given in Fig. 1, along with

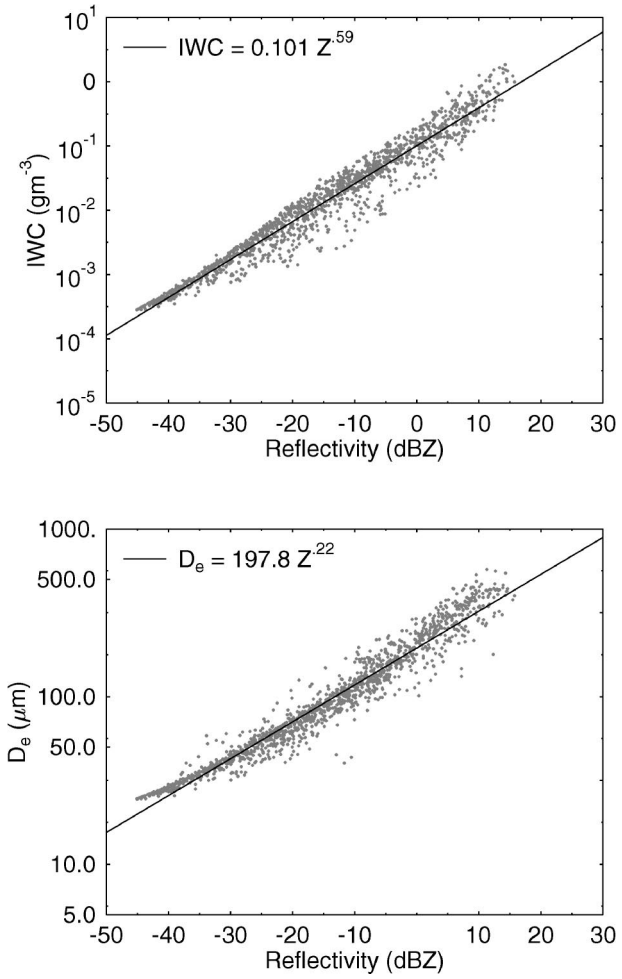

FIG. 1. Retrieved IWC and D_e from CEPEX data as a function of calculated radar reflectivity plus regression lines.

best-fit curves to the equations IWC = aZ_e^b and $D_e = cZ_e^d$. The best-fit regression equation for IWC compares very well to that given by Liu and Illingworth (2000) for CEPEX data at 35 GHz, which is IWC = $0.0977Z_e^{0.596}$. To reduce the scatter in the regression relationships, we stratify the observations by temperature and calculate regression equations for IWC/Z_e and D_e/Z_e for each 5°C bin from −70° to −10°C. Following Brown et al. (1995) we estimate the uncertainty in the regression equations for several values of reflectivity and find approximately a factor of 1.4 uncertainty in the regression of ice water content and a factor of 1.15 uncertainty in the regression of effective diameter for a given reflectivity. This uncertainty represents the factor by which you can multiply or divide the mean value of IWC or effective diameter for a given reflectivity value in order to include ~68% of the observations. Other sources of error in the ice cloud property retrievals include the representativeness of the CEPEX data and the errors in calculating the IWC and reflectivity from the 2DC data. Unfortunately, little is known about how representative the CEPEX data is of the cirrus at Nauru, as no in situ measurements of cirrus microphysical properties over Nauru are available.

c. Data quality issues

A peak in the MWR brightness temperatures around local solar noon was noticed during the periods 14 September–6 October 1999 and 7 March–30 March 2000. This peak in brightness temperatures appears to be due to solar contamination of the MWR signal around the equinox periods, at which times the sun would be directly overhead around solar noon at Nauru. Data from the MWR for the 2 h around noon during these periods are not used. The MMCR had sporadic problems throughout the study period, the longest being a time period between 20 December 1999 and 17 January 2000 in which the radar data were invalid.

3. Retrieved cloud properties

Over the period 1 June 1999 through 31 May 2000 there were over 2.5 million valid radar observations. Cloud properties were not retrieved during times of precipitation (optical rain gauge values >0.05 mm h^{-1}), which occurred 1.2% of the time. In Table 1 we show the percentage of time liquid clouds, ice clouds, and clear sky that were detected by the radar for each month of the study. There is considerable variability in the percentage of clouds detected throughout the study period that may be associated with the Madden–Julian oscillation, which is a major mode of intraseasonal variability in the Tropics (Madden and Julian 1994). The month of May 2000 has a very high frequency of precipitating clouds and a very low frequency of cloudless columns, while the period of September through December 1999 has the lowest percentage of precipitating clouds and the highest frequency of cloudless columns. The months of February through April 2000 have very low frequency of radar detected cirrus clouds relative to the other months. Based on examination of images of high cloud cover amount developed from Geostationary Meteorological Satellite (GMS) imagery at NASA Langley (available online at http://www-pm.larc.narsa.gov/arm/TWP/arm-twp.html), this decrease in cirrus amount is a real phenomenon and not a problem with the cloud radar.

a. Liquid clouds

The nonprecipitating liquid clouds at Nauru are most often shallow trade cumulus. The average base of the liquid clouds is 849 m, and the average top height is 1340 m. Figure 2 shows a histogram of the heights of the bases and tops of the liquid clouds over the study period. The distributions show a strong peak at low heights and then a long tail toward higher clouds. The long tail may skew the representativeness of the average

TABLE 1. Statistics of cloud retrievals.

Month	No. of valid columns	Percentage of time each cloud type detected				
		Precipitation	Liquid	Ice	Liquid and ice	No cloud
Jun 1999	251 873	0.9	22.5	21.9	9.55	45.1
Jul 1999	265 249	1.1	19.9	25.8	9.4	43.8
Aug 1999	266 785	2.0	21.4	20.6	8.3	47.8
Sep 1999	258 768	0.3	24.6	12.4	5.0	57.7
Oct 1999	239 441	1.2	27.8	12.2	7.7	51.2
Nov 1999	249 420	0.2	21.4	19.1	6.9	52.4
Dec 1999	155 457	0.1	29.2	12.7	6.9	51.1
Jan 2000	118 121	0.2	16.3	30.0	15.3	38.2
Feb 2000	234 563	0.5	36.8	7.9	4.3	50.4
Mar 2000	258 535	0.9	37.8	9.5	5.4	46.4
Apr 2000	216 000	1.3	36.1	11.0	6.4	45.2
May 2000	159 200	6.2	29.3	15.4	11.3	37.7
All data	2 773 492	1.2	26.9	16.4	7.7	47.9

values. The median base height for the liquid clouds is 611 m, and the median top height is 1010 m. The few cases with very low base heights could be due to precipitation contamination of the radar reflectivities. Eighty-five percent of the liquid clouds have bases below 1 km, and 89% have tops less than 2 km.

The shallow cumulus clouds at Nauru have relatively low liquid water paths (LWPs) and optical depths. Figure 3 shows the cumulative distribution functions for the retrieved LWP and optical depths of the liquid clouds. Approximately 90% of the retrieved liquid clouds have a liquid water path less than 100 g m^{-2} and optical depths less than 16. The mean LWP over the study period is 42.7 g m^{-2} with a standard deviation of 86.1 g m^{-2} and the mean optical depth is 7.2 with a standard deviation of 11.0. The average uncertainties in the Bayesian retrievals are 14.4 g m^{-2} for LWP and 2.9 for optical depth.

Figure 4 shows the effective radius and liquid water content distributions for the retrieved liquid clouds. The mean effective radius over the study period is 7.5 μm, with a standard deviation of 3.2 μm and an average Bayesian retrieval uncertainty of 0.4 μm. The mean retrieved liquid water content for cloudy range gates is 0.092 g m^{-3}, with a standard deviation of 0.13 g m^{-3}, and an average Bayesian retrieval uncertainty of 0.05 g m^{-3}. The distribution of LWC has a very long tail with a significant number of range gates having values of LWC higher than 0.30 g m^{-3}. These retrieved values are typical of the microphysical properties of shallow cumulus clouds retrieved from in situ aircraft obser-

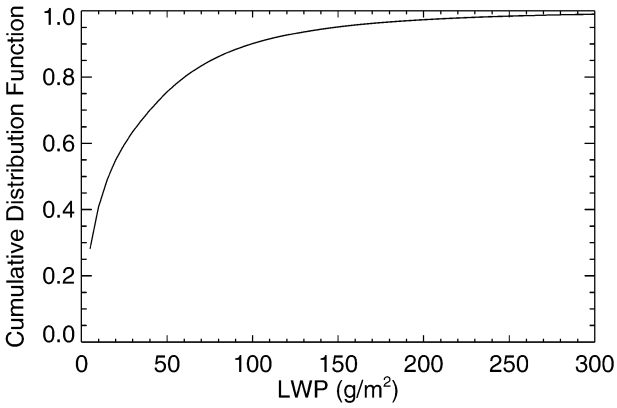

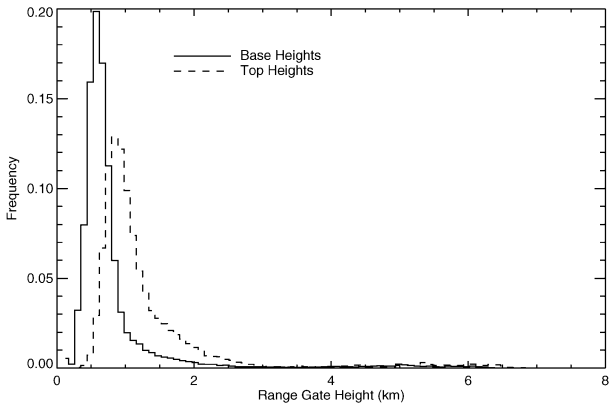

FIG. 2. Histogram of base and top heights of liquid clouds at Nauru.

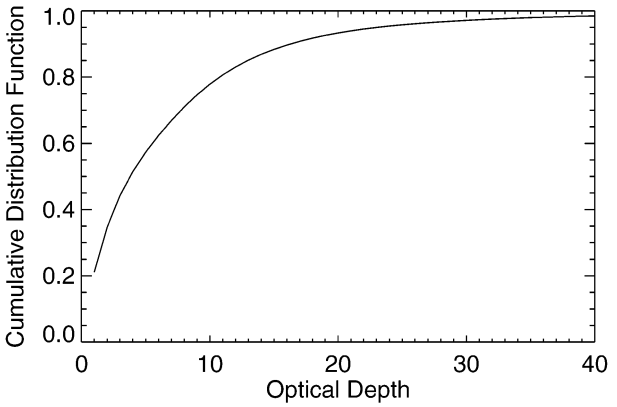

FIG. 3. Cumulative distribution function of (a) LWP and (b) optical depth for retrieved liquid clouds at Nauru.

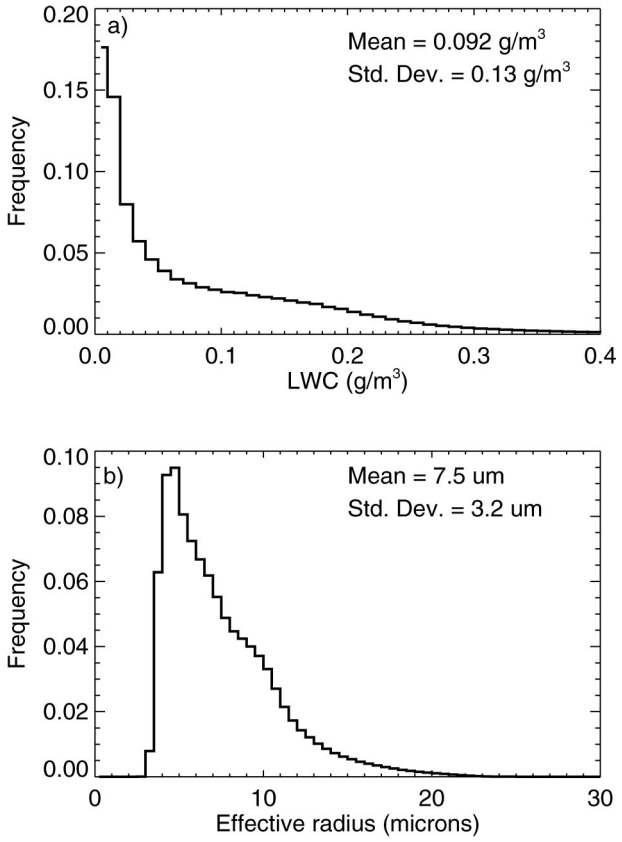

FIG. 4. Histograms of (a) LWC and (b) effective radius for retrieved liquid clouds at Nauru.

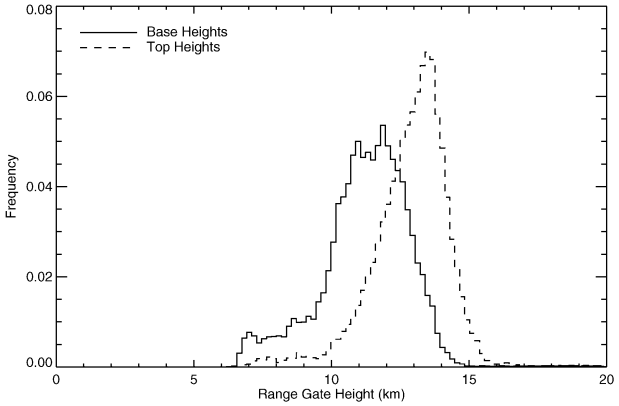

FIG. 5. Histogram of base and top heights of ice clouds at Nauru.

vations. In shallow cumulus off the coasts of Hawaii and Australia, Squires (1956) and Squires and Warner (1957) found average median radii of 6.5–10 μm and average liquid water contents of 0.08–0.5 g m^{-3} per cloud penetration. From a series of aircraft measurements taken in trade wind cumulus clouds east of Cairns, Australia, Stephens and Platt (1987) characterize the clouds as having effective radii ranging from 4 μm at cloud base to greater than 10 μm at cloud top, and having liquid water contents generally less than 0.3 g m^{-3}. The large uncertainty in the Bayesian retrievals of LWC and LWP are due primarily to the lack of sensitivity of the MWR to shallow clouds with low liquid water paths. Although the MWR was found to be accurate to within $\pm$ 1 K during the Nauru99 field experiment, a difference of 1 K in measured brightness temperature at 31.4 GHz corresponds to a change of $\sim$30 g m^{-2} in liquid water path.

b. Ice clouds

Due to the failure of the MPL in November 1999, we did not use the MPL in the detection of cloud occurrence in this study. This probably leads to an overestimate of the amount of clear sky as the MMCR has been shown to miss thin clouds composed of small particles, such as tenuous tropopause cirrus (Clothiaux et al. 2000). To estimate the amount of thin cloud missed by the MMCR, we look at the MPL cloud bases retrieved from the Clothiaux et al. (1998) algorithm for the period June–October 1999. In general, clouds were detected in the MPL observations for about 20% of the time in which no clouds were detected in the MMCR observations. These clouds tend to be high, thin cirrus with low optical depths. Although they may have local impacts on the heating rate and outgoing longwave radiation, their impact on the surface fluxes will be relatively small, therefore we neglect them for the closure study.

Figure 5 shows a histogram of the heights of the bases and tops of the radar detected cirrus clouds over the study period. The mean base height for the cirrus clouds is 11.2 km, and the average top height is 12.9 km. However, the radar may not detect the true top of the cirrus clouds due to low reflectivities from very small particles at the top of the clouds. Clothiaux et al. (2000) compared cloud-base detections from the MMCR to those from lidar and ceilometer at the ARM Southern Great Plains site in Oklahoma and found that the percentage of cirrus not detected by the MMCR increased with the height of the laser-derived cloud base. In an analysis of airborne lidar data from TOGA COARE, Sassen et al. (2000) found similar cirrus-base heights to those presented here, but the cirrus cloud tops were generally $\sim$2 km higher, often extending to the tropopause (which had an average height of 16.85 km).

Figure 6 shows a histogram of the retrieved IWP of the radar-detected ice clouds. The mean IWP over the study period is 22.1 g m^{-2} with a standard deviation of 72.9 g m^{-2}, indicating the large variability in the cirrus clouds. Figure 7 shows a histogram of the retrieved ice water content and effective diameter of the cirrus clouds. The mean IWC is 0.014 g m^{-3} and the mean D_e is 72 μm. Unfortunately, few observations of cirrus microphysics in the Tropics exist for comparison to these retrievals. Measurements taken near Kwajalein, Marshall Islands, in the 1970s and measurements during CEPEX show that the mean values of the retrieved IWC

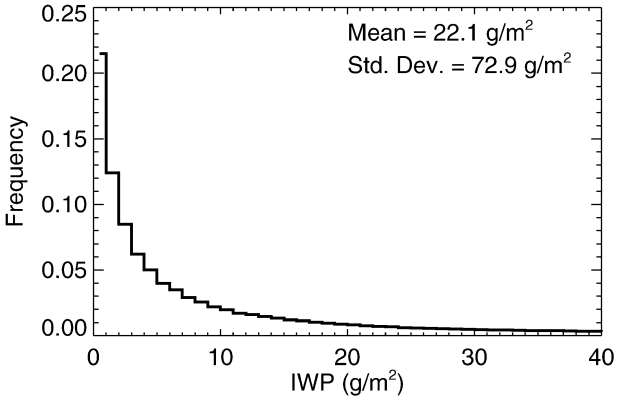

FIG. 6. Histogram of ice water path for retrieved ice clouds at Nauru.

and D_e are not unreasonable for tropical cirrus clouds. The median IWC measured from aircraft in situ microphysical probes during these experiments ranged from 0.004 to 0.1 g m^{-3} for layers with temperatures from $-70°$ to $-20°$C. The median effective diameters ranged from 60 to 440 μm over the same temperature range (Heymsfield and McFarquhar 1996).

4. Diurnal variability

To examine the diurnal variability of the retrieved cloud occurrence and cloud properties, the retrieved variables are averaged over each hour of the day over the entire dataset. Figure 8 shows the frequency of liquid cloud detection as a function of time of day. Daylight hours are indicated by the lighter bars. There is a marked increase in the percentage of times liquid clouds are detected during the daylight hours. Between 0600 and 1800 local standard time (LST), liquid clouds are detected 40.1% of the time on average, while they are detected only 29.0% of the time after 1800 LST. The increase in cloud frequency during the day is due in part to the island cloud effect. During the Nauru99 field experiment, cloud plumes starting near the ARCS site and advecting downwind with the prevailing easterly trade winds were frequently observed (Nordeen et al. 2001). The formation of these clouds is believed to be due primarily to diurnal heating of the island. Observations during the Nauru99 experiment showed that the island air temperature was similar to the ocean air temperature at midnight, but at 1030 LST, the island was roughly 4.5°C warmer than the surrounding ocean (Nordeen et al. 2001).

The diurnal cycle is also seen in some of the retrieved cloud properties. Figure 9 shows the average retrieved optical depth, cloud base, and cloud thickness for liquid clouds as a function of time of day. During the daylight hours the average optical depth is 6.9, which is 10% less than the average values of 7.5 during nighttime hours, and the average cloud base is significantly lower (781 m during the day versus 943 m at night), while

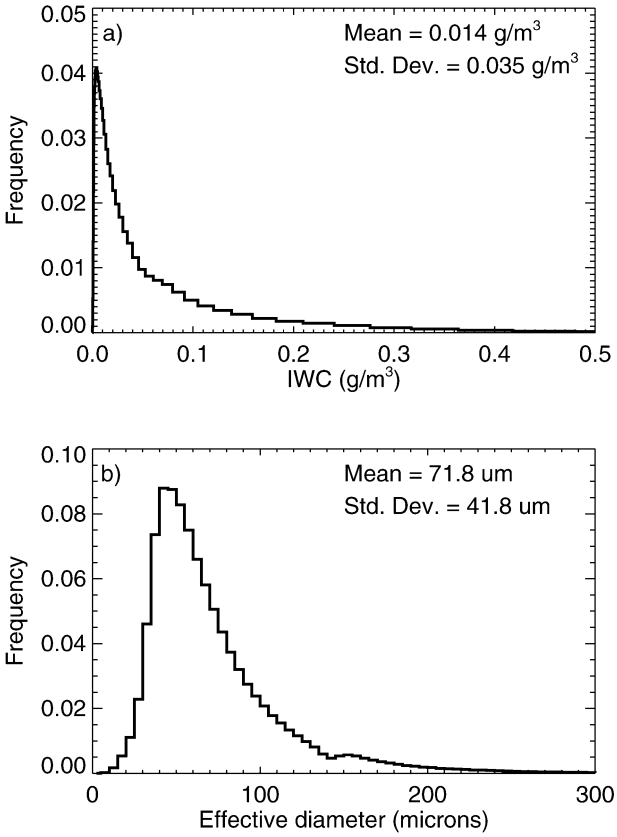

FIG. 7. Histogram of (a) ice water content and (b) effective diameter retrieved for ice clouds at Nauru.

the cloud thickness does not show a clear trend. The average cloud-base height is roughly constant during the daylight hours after 1030 LST when the local lifting condensation level is roughly constant. The average cloud-base height increases in the late afternoon and evening to a maximum near 2300 LST and then decreases again. The increase in cloud-base height in the

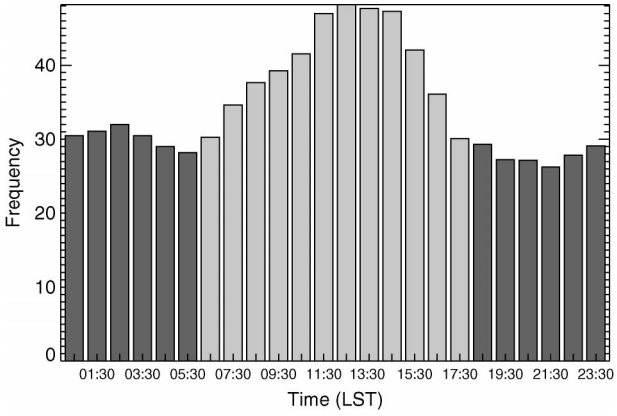

FIG. 8. Average frequency of detection of liquid clouds by the cloud radar as a function of time of day. Lighter-shaded bars represent daylight hours.

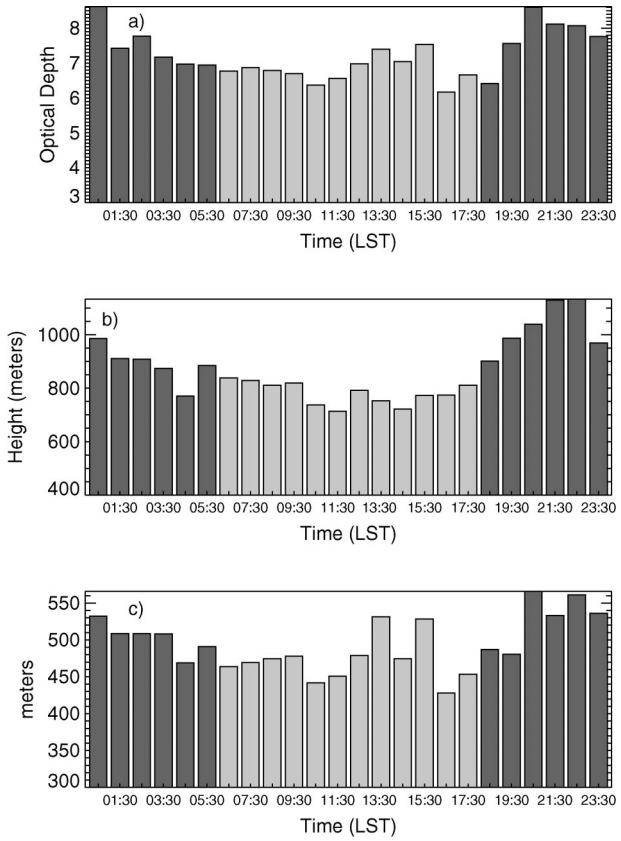

FIG. 9. Average retrieved (a) optical depth, (b) cloud-base height, and (c) cloud thickness for liquid clouds as a function of time of day.

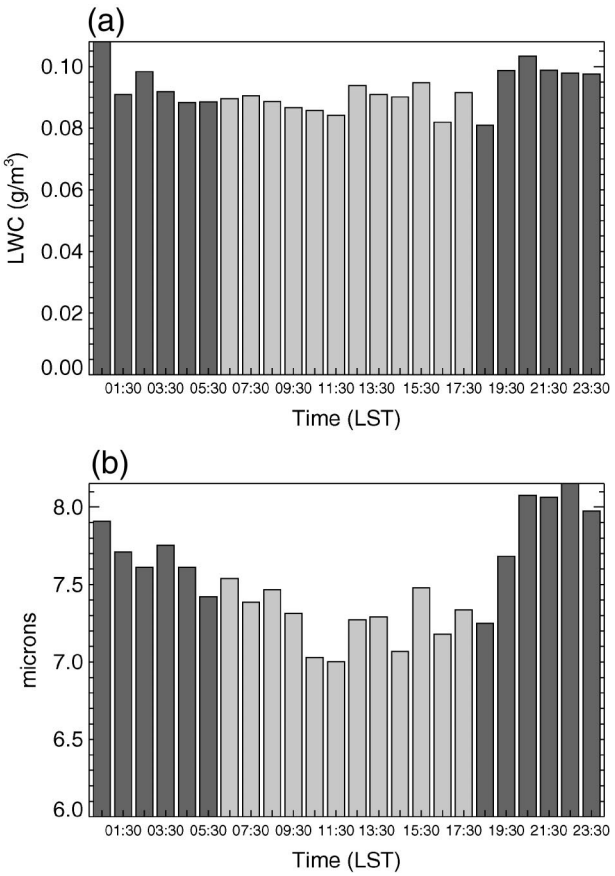

FIG. 10. Average retrieved (a) LWC and (b) effective radius for liquid clouds as a function of time of day.

evening may be due to the gradual decay of the initial cloud bases from entrainment and the continued buoyancy of the original cloud elements even as the convection and initiation of new clouds is shut off, or to less evaporation and lower boundary layer mixing ratios at night. Figure 10 shows the average retrieved liquid water content and effective radius as a function of time of day. The average effective radius is smaller during the day, with an average value of 7.3 μm, compared to 7.7 μm at night, while there is no significant difference in the liquid water content between daylight and night hours. Comparison of the diurnal variability calculated using the entire dataset and calculated by leaving out the dates where data from the MWR were not available around noon showed no significant difference.

In contrast to the liquid clouds, ice clouds are more frequently detected in the evening and predawn hours. Figure 11 shows the frequency of the radar-detected ice clouds as a function of time of day. As in the previous set of figures, daylight hours are indicated by the lighter bars. During the daylight hours, between 0600 and 1800 LST, ice clouds are detected 21.9% of the time on average, while they are detected 26.1% of the time after 1800 LST.

The ice clouds detected by the radar are primarily associated with outflow from convective anvils. The increased frequency of ice cloud detection at night is consistent with previous studies of cold cloud over the tropical oceans from satellite data, which generally show a maximum in cold cloud amount before dawn (Fu et al. 1990; Janowiak et al. 1994; Chen and Houze 1997). Fu et al. (1990) examined the diurnal variability in cloud-

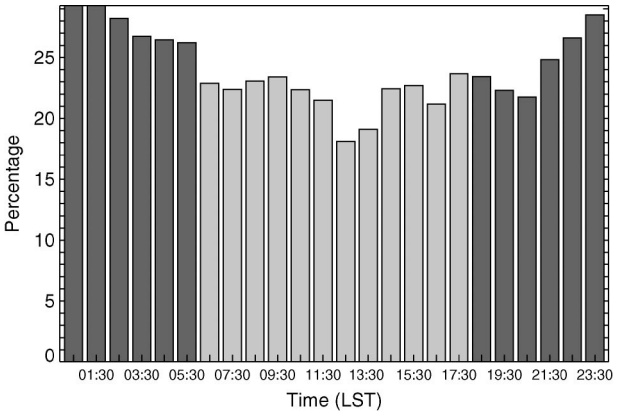

FIG. 11. Average frequency of detection of ice clouds by the cloud radar.

iness derived from ISCCP radiances over the equatorial Pacific oceanic regions. They separate cold clouds into deep convective clouds (DCC) and cirrus/anvil clouds (CAC). In their study, DCC covered only 2% of the region, while CAC covered ~21%. Diurnal variability in the two types were out of phase with DCC peaking in the morning and CAC peaking in the early evening. Similarly, Chen and Houze (1997) conclude that the diurnal cycle of cloud cover over the oceans is a combination of diurnal radiative forcing (which initiates the convection) and the life cycle of the convection, with large convective systems taking 6–12 h to reach their maximum areal coverage. Unlike the liquid clouds, there are no clear diurnal trends in the ice cloud properties.

5. Summary and conclusions

Microphysical properties of nonprecipitating liquid and ice clouds were retrieved from 12 months of millimeter wave radar and microwave radiometer measurements at Nauru. Liquid cloud properties were retrieved using the Bayesian method of McFarlane et al. (2002) and ice cloud properties were retrieved from regression equations based on in situ data from the CEPEX experiment, which relate radar reflectivity to ice water content and effective diameter. Due to difficulties in maintaining instruments at remote tropical sites, there were gaps of various lengths in the dataset. However, cloud properties were retrieved for roughly 11 months, a much longer time series than previously available in the TWP region.

Liquid water clouds observed at Nauru were generally shallow trade wind cumulus, with bases below 1 km and tops below 2 km. The mean retrieved liquid water path was 42.7 g m^{-2} and approximately 90% of the retrieved liquid clouds had liquid water paths less than 100 g m^{-2}. The mean retrieved effective radius was 7.5 μm, and mean retrieved liquid water content was 0.092 g m^{-3}, although the lack of sensitivity of the microwave radiometer led to large uncertainties in retrieved liquid water content for the shallow clouds typically seen at Nauru. The frequency of liquid cloud detection and height of the liquid cloud base showed a clear diurnal cycle, which is most likely related to the island effect and the existence of the Nauru cloud plume.

Island-induced cloud plumes are not unique to Nauru and have been observed downwind of other islands in satellite images (Nordeen et al. 2001). However, the island-induced clouds may bias the observations at Nauru relative to the surrounding ocean. Recently, a suite of instruments was installed on the upwind side of Nauru as part of the Nauru Island Effects Study (Widener and Long 2002). Analysis of this data should help our understanding of the frequency of the island effect and the magnitude of its influence on the cloud amount and radiation budget at Nauru.

During the study, ice clouds with no underlying liquid clouds were detected in 16.4% of the radar observations and ice clouds above liquid clouds 7.7% of the time. The mean retrieved IWP of the radar-detected ice clouds was 22.1 g m^{-2} and the mean effective diameter retrieved was 72 μm. Large monthly variability was seen in both the amount of cirrus detected and the retrieved ice water path. Ice clouds were observed by the radar more frequently at night than during the day at Nauru, but there was no clear diurnal trend in the retrieved microphysical properties. Thin cirrus clouds, which were detected by the lidar but not the radar were observed roughly 20% of the time that the micropulse lidar was operational. Since the lidar cannot detect this thin cirrus if underlying liquid or ice clouds exist, the true frequency is probably higher. For example, McFarquhar et al. (2000) found that tropopause cirrus (defined as cirrus with bases and tops greater than 15 km) occurred 29% of the time during CEPEX, with thick cirrus observed below the tropopause cirrus 43% of the time.

In Part II of this paper, this dataset will be used to examine whether the retrieved cloud properties are consistent with the observed surface radiation at Nauru.

Acknowledgments. The authors thank Dr. Roger Marchand, Dr. Chuck Long, and three anonymous reviewers for their helpful comments on the manuscript. This research was supported by the Office of Biological and Environmental Research of the U.S. Department of Energy (under Grant DE-A1005-90ER61069 to the NASA Goddard Space Flight Center) as part of the Atmospheric Radiation Measurement program. S. McFarlane was supported in part by a National Science Foundation Graduate Research Fellowship. Data were obtained from the Atmospheric Radiation Measurement program sponsored by the U.S. Department of Energy, Office of Science, Office of Biological and Environmental Research, Environmental Sciences Division.

REFERENCES

Albrecht, B. A., 1981: Parameterization of trade-cumulus cloud amounts. *J. Atmos. Sci.,* **38,** 97–105.

Atlas, D., S. Y. Matrosov, A. J. Heymsfield, M.-D. Chouh, and D. B. Wolff, 1995: Radar and radiation properties of ice clouds. *J. Appl. Meteor.,* **34,** 2329–2345.

Brown, P. R., A. J. Illingworth, A. J. Heymsfield, G. M. McFarquhar, K. A. Browning, and M. Gosset, 1995: The role of spaceborne millimeter-wave radar in the global monitoring of ice cloud. *J. Appl. Meteor.,* **34,** 2346–2366.

Chen, S. S., and R. A. Houze, 1997: Diurnal variation and life-cycle of deep convective systems over the tropical Pacific warm pool. *Quart. J. Roy. Meteor. Soc.,* **123,** 357–388.

Clothiaux, E. E., G. G. Mace, T. P. Ackerman, T. J. Kane, J. D. Spinhirne, and V. S. Scott, 1998: An automated algorithm for detection of hydrometeor returns in micropulse lidar data. *J. Atmos. Oceanic Technol.,* **15,** 1035–1042.

——, and Coauthors, 1999: The Atmospheric Radiation Measurement program cloud radars: Operational modes. *J. Atmos. Oceanic Technol.,* **16,** 819–827.

——, T. P. Ackerman, G. G. Mace, K. P. Moran, R. T. Marchand, M. A. Miller, and B. E. Martner, 2000: Objective determination of cloud heights and radar reflectivities using a combination of active remote sensors at the Atmospheric Measurement Program

Cloud and Radiation Test Bed (ARM CART) sites. *J. Appl. Meteor.*, **39,** 645–665.
Comstock, J. M., and K. Sassen, 2001: Retrieval of cirrus cloud radiative and backscattering properties using combined lidar and infrared radiometer (LIRAD) measurements. *J. Atmos. Oceanic Technol.*, **18,** 1658–1673.
Dong, X., T. P. Ackerman, E. E. Clothiaux, P. Pilewskie, and Y. Han, 1997: Microphysical and radiative properties of boundary layer stratiform clouds deduced from ground-based measurements. *J. Geophys. Res.*, **102,** 23 829–23 843.
Duynkerke, P. G., 1998: Dynamics of cloudy boundary layers. *Clear and Cloudy Boundary Layers*, A. A. M. Holtslag and P. G. Duynkerke, Eds., Royal Netherlands Academy of Arts and Sciences, 199–218.
French, J. R., G. Vali, and R. D. Kelly, 2000: Observations of microphysics pertaining to the development of drizzle in warm, shallow cumulus clouds. *Quart. J. Roy. Meteor. Soc.*, **126,** 415–443.
Frisch, A. S., C. W. Fairall, and J. B. Snider, 1995: Measurement of stratus cloud and drizzle parameters in ASTEX with a Ka-band Doppler radar and a microwave radiometer. *J. Atmos. Sci.*, **52,** 2788–2799.
——, G. Feingold, C. W. Fairall, T. Uttal, and J. B. Snider, 1998: On cloud radar and microwave radiometer measurements of stratus cloud liquid water profiles. *J. Geophys. Res.*, **103,** 23 195–23 197.
Fu, R., A. D. Del Genio, and W. B. Rossow, 1990: Behavior of deep convective clouds in the tropical Pacific deduced from ISCCP radiances. *J. Climate*, **3,** 1129–1152.
Han, Y., and E. R. Westwater, 2000: Analysis and improvement of tipping calibration for ground-based microwave radiometers. *IEEE Trans. Geosci. Remote Sens.*, **38,** 1–18.
Heymsfield, A. J., and G. M. McFarquhar, 1996: High albedos of cirrus in the tropical Pacific warm pool: Microphysical interpretations from CEPEX and from Kwajalein, Marshall Islands. *J. Atmos. Sci.*, **53,** 2424–2450.
——, K. M. Miller, and J. D. Spinhirne, 1990: The 27–28 October 1986 FIRE IFO cirrus case study: Cloud microstructure. *Mon. Wea. Rev.*, **118,** 2313–2328.
Intrieri, J. M., G. L. Stephens, W. L. Eberhard, and T. Uttal, 1993: A method for determining cirrus cloud particle sizes using lidar and radar backscatter technique. *J. Appl. Meteor.*, **32,** 1074–1082.
Janowiak, J. E., P. A. Arkin, and M. Morrissey, 1994: An examination of the diurnal cycle in oceanic tropical rainfall using satellite and in situ data. *Mon. Wea. Rev.*, **122,** 2296–2311.
Liao, L., and K. Sassen, 1994: Investigation of relationships between Ka-band radar reflectivity and ice and liquid water contents. *Atmos. Res.*, **34,** 231–248.
Liu, C.-L., and A. J. Illingworth, 2000: Toward more accurate retrievals of ice water content from radar measurements of clouds. *J. Appl. Meteor.*, **39,** 1130–1146.
Mace, G. G., and K. Sassen, 2000: A constrained algorithm for retrieval of stratocumulus cloud properties using solar radiation, microwave radiometer, and millimeter cloud radar data. *J. Geophys. Res.*, **105,** 29 099–29 108.
——, T. Ackerman, P. Minnis, and D. Young, 1998: Cirrus layer microphysical properties derived from surface-based millimeter radar and infrared interferometer data. *J. Geophys. Res.*, **103,** 23 207–23 216.
——, A. J. Heymsfield, and M. R. Poellot, 2002: On retrieving the microphysical properties of cirrus clouds using the moments of the millimeter-wavelength Doppler spectrum. *J. Geophys. Res.*, **107**, 4815, doi:10.1029/2001JD001308.
Madden, R., and P. Julian, 1994: Observations of the 40–50-day tropical oscillation—A review. *Mon. Wea. Rev.*, **122,** 814–837.
Mather, J., T. Ackerman, W. Clements, F. Barnes, M. Ivey, L. Hatfield, and R. Reynolds, 1998: An atmospheric radiation and cloud station in the tropical western Pacific. *Bull. Amer. Meteor. Soc.*, **79,** 627–642.
Matrosov, S. Y., B. W. Orr, R. A. Kropfli, and J. B. Snider, 1994: Retrieval of vertical profiles of cirrus cloud microphysical parameters from Doppler radar and infrared radiometer measurements. *J. Appl. Meteor.*, **33,** 617–626.
——, A. J. Heymsfield, R. A. Kropfli, B. E. Martner, R. F. Reinking, J. B. Snider, P. Piironen, and E. W. Eloranta, 1998: Comparisons of ice cloud parameters obtained by combined remote sensor retrievals and direct methods. *J. Atmos. Oceanic Technol.*, **15,** 184–196.
——, A. Korolev, and A. J. Heymsfield, 2002: Profiling ice mass and characteristic particle size from Doppler radar measurements. *J. Atmos. Oceanic Technol.*, **19,** 1003–1018.
McFarlane, S. A., K. F. Evans, and A. S. Ackerman, 2002: A Bayesian algorithm for the retrieval of liquid water cloud properties from microwave radiometer and millimeter radar data. *J. Geophys. Res.*, **107**, 4317, doi:10.1029/2001JD001011.
McFarquhar, G. M., and A. J. Heymsfield, 1996: Microphysical characteristics of three anvils sampled during the Central Equatorial Pacific Experiment. *J. Atmos. Sci.*, **53,** 2401–2423.
——, and ——, 1997: Parameterization of tropical cirrus ice crystal size distributions and implications for radiative transfer: Results from CEPEX. *J. Atmos. Sci.*, **54,** 2187–2200.
——, ——, J. Spinhirne, and B. Hart, 2000: Thin and subvisual tropopause tropical cirrus: Observations and radiative impacts. *J. Atmos. Sci.*, **57,** 1841–1853.
Moran, K. P., B. E. Martner, D. Welsh, D. Merritt, M. Post, and T. Uttal, 1997: ARM's cloud profiling radar. Preprints, *28th Int. Conf. on Radar Meteorology*, Austin, TX, Amer. Meteor. Soc., 296–297.
Nordeen, M. L., P. Minnis, D. R. Doelling, D. Pethick, and L. Nguyen, 2001: Satellite observations of cloud plumes generated by Nauru. *Geophys. Res. Lett.*, **28,** 631–634.
Raga, G. B., J. B. Jensen, and M. B. Baker, 1990: Characteristics of cumulus band clouds off the coast of Hawaii. *J. Atmos. Sci.*, **47,** 338–355.
Ramanathan, V., and W. Collins, 1991: Thermodynamic regulation of ocean warming by cirrus clouds deduced from observations of the 1987 El Niño. *Nature*, **351,** 27–32.
Randall, D. A., Q. Shao, and M. Branson, 1998: Representation of cloudy boundary layers in climate models. *Clear and Cloudy Boundary Layers*, A. A. M. Holtslag and P. G. Duynkerke, Eds., Royal Netherlands Academy of Arts and Sciences, 305–322.
Sassen, K., G. G. Mace, Z. Wang, M. R. Poellot, S. M. Sekelsky, and R. E. McIntosh, 1999: Continental stratus clouds: A case study using coordinated remote sensing and aircraft measurements. *J. Atmos. Sci.*, **56,** 2345–2358.
——, R. P. Benson, and J. D. Spinhirne, 2000: Tropical cirrus cloud properties derived from TOGA/COARE airborne polarization lidar. *Geophys. Res. Lett.*, **27,** 673–676.
Schneider, T. L., and G. Stephens, 1995: Theoretical aspects of modeling backscattering by cirrus ice particles at millimeter wavelengths. *J. Atmos. Sci.*, **52,** 4367–4385.
Squires, P., 1956: The micro-structure of cumuli in maritime and continental air. *Tellus*, **8,** 443–444.
——, and J. Warner, 1957: Some measurements in the orographic cloud of the island of Hawaii and in trade wind cumuli. *Tellus*, **9,** 475–494.
Stephens, G. L., and C. M. R. Platt, 1987: Aircraft observations of the radiative and microphysical properties of stratocumulus and cumulus cloud fields. *J. Climate Appl. Meteor.*, **26,** 1243–1269.
Wang, Z., and K. Sassen, 2002: Cirrus cloud microphysical property retrieval using lidar and radar measurements. Part I: Algorithm description and comparison with in situ data. *J. Appl. Meteor.*, **41,** 218–229.
Webster, P. J., and R. Lukas, 1992: The Coupled Ocean–Atmosphere Response Experiment. *Bull. Amer. Meteor. Soc.*, **73,** 1377–1416.
——, C. A. Clayson, and J. A. Curry, 1996: Clouds, radiation, and the diurnal cycle of sea surface temperature in the tropical western Pacific. *J. Climate*, **9,** 1712–1730.

Westwater, E. R., and Coauthors, 1999: Ground-based remote sensor observations during PROBE in the tropical western Pacific. *Bull. Amer. Meteor. Soc.*, **80,** 257–270.

——, B. B. Stankov, D. Cimini, Y. Han, J. A. Shaw, B. M. Lesht, and C. N. Long, 2003: Radiosonde humidity soundings and microwave radiometers during Nauru99. *J. Atmos. Oceanic Technol.*, **20,** 953–971.

Widener, K. B., and C. N. Long, cited 2002: Nauru Island effect study—Installation and preliminary data. *Proc. 12th Atmospheric Radiation Measurement Program Science Team Meeting*, St. Petersburg, FL, U.S. Department of Energy. [Available online at http://www.arm.gov/docs/documents/technical/conf_0204/widener(1)-kb.pdf.]

Yang, P., K. N. Liou, K. Wyser, and D. Mitchell, 2000: Parameterization of the scattering and absorption properties of individual ice crystals. *J. Geophys. Res.*, **105,** 4699–4718.